Original Article

KLF7 promotes preadipocyte proliferation via activation of the Akt signaling pathway by *Cis*-regulating CDKN3

Ziqiu Jia, Zhao Jin, Shuli Shao, Hu Xu, Wen Li, Mahmood Khan, Weiyu Wang, Weiwei Zhang, and Yingning Sun*

College of Life Science and Agriculture Forestry, Qiqihar University, Qiqihar 161006, China
*Correspondence address. Tel: +86-452-2742704; E-mail: SunYN@qqhru.edu.cn

Abstract

Krüppel-like transcription factor 7 (KLF7) promotes preadipocyte proliferation; however, its target gene in this process has not yet been identified. Using KLF7 ChIP-seq analysis, we previously showed that a KLF7-binding peak is present upstream of the cyclin-dependent kinase inhibitor 3 gene (*CDKN3*) in chicken preadipocytes. In the present study, we identify *CDKN3* as a target gene of KLF7 that mediates the effects of KLF7 on preadipocyte proliferation. Furthermore, 5′-truncating mutation analysis shows that the minimal promoter is located between nt −160 and nt −7 (relative to the translation initiation codon ATG) of *CDKN3*. KLF7 overexpression increases *CDKN3* promoter activity in the DF-1 and immortalized chicken preadipocyte (ICP1) cell lines. Deletion of the putative binding site of KLF7 abolishes the promotive effect of KLF7 overexpression on *CDKN3* promoter activity. Moreover, *CDKN3* knockdown and overexpression assays reveal that *CDKN3* enhances ICP1 cell proliferation. Flow cytometry analysis shows that *CDKN3* accelerates the G1/S transition. Furthermore, we find that KLF7 promotes ICP1 cell proliferation via Akt phosphorylation by regulating *CDKN3*. Taken together, our results suggest that KLF7 promotes preadipocyte proliferation by activating the Akt signaling pathway by *cis*-regulating *CDKN3*, thus driving the G1/S transition.

Key words proliferation, cyclin-dependent kinase inhibitor 3, Krüppel-like transcription factor 7, Akt signaling pathway, preadipocyte

Introduction

In recent years, the incidences of type 2 diabetes, coronary heart disease, and other obesity-related diseases have increased rapidly, and these diseases have become a major public health problem [1]. Obesity is mainly caused by excessive fat deposition [2], which is associated with an increase in the number and size of adipocytes. Adipocyte number is mainly attributed to preadipocyte proliferation, whereas adipocyte size is attributed to preadipocyte differentiation [3]. Preadipocyte proliferation is a complex process controlled by a regulatory network of multiple factors, including transcription factors [4–6], cytokines [7], and noncoding RNAs [8,9].

Krüppel-like transcription factors (KLFs) are essential for many physiological and pathological processes [10,11]. KLF7 is associated with obesity [12,13], type 2 diabetes [14], and cardiovascular and cerebrovascular diseases [15,16]. KLF7 inhibits preadipocyte differentiation in mammals and birds [4,17] and promotes chicken preadipocyte proliferation [4]. In isolated chicken stromal-vascular cells, KLF7-overexpressing cells exhibited an increased proliferation ability, especially at 48 h and 120 h after transfection, when compared with the control cells [4]. The negative effect of KLF7 on preadipocyte differentiation is mainly achieved via the regulation of target genes such as *GATA3* [18] and *HIF1A* [19]. However, the target gene of KLF7 in the process of promoting chicken preadipocyte proliferation remains unknown.

Chicken is an ideal model for studying adipogenesis, obesity, and adipose biology [20–22]. In our previous study, ChIP-seq analysis of chicken preadipocytes revealed a KLF7-binding peak upstream of the cyclin-dependent kinase inhibitor 3 (*CDKN3*) gene, implying that *CDKN3* may be a direct target gene of KLF7 (data not shown). Given that *CDKN3* is a cell cycle regulator [23], in this study, we aimed to investigate the function of *CDKN3* in preadipocyte proliferation and whether it mediates the role of KLF7 in preadipocytes. We characterized the structure of the *CDKN3* promoter and found that KLF7 regulates *CDKN3* expression. In addition, we explored the role and molecular mechanism of *CDKN3* in preadipocyte proliferation. Our results showed that KLF7

promotes preadipocyte proliferation by activating the Akt pathway, which subsequently accelerates the G1/S transition via the upregulation of CDKN3 transcription. To the best of our knowledge, this study is the first to reveal the mechanism by which KLF7 upregulates preadipocyte proliferation.

Materials and Methods

Animals and tissue sampling

Abdominal fat tissue samples were obtained from Arbor Acres (AA) commercial broilers (Aviagen Broiler Breeders, Beijing, China). In total, 21 birds (3 birds per time point) were sacrificed at 1–7 weeks of age. Abdominal fat tissues were collected, snap-frozen and stored in liquid nitrogen until RNA extraction.

The animal experiment was performed following the guidelines issued by the Ministry of Science and Technology of China (approval number: 2006-398) and was approved by the Laboratory Animal Management Committee of Qiqihar University.

Cell lines and culture

The immortalized chicken preadipocyte ICP1 [24] and chicken fibroblast DF-1 [25] cell lines were kindly provided by the Key Laboratory of Chicken Genetics and Breeding, Ministry of Agriculture and Rural Affairs, Northeast Agricultural University (Harbin, China). ICP1 cells have been widely used to study chicken adipogenesis [26,27], as they present the same morphological and differentiation characteristics as primary preadipocytes [24,26,27]. DF-1, an immortalized chicken fibroblast cell line, can be easily transiently transfected with exogenous DNA. DF-1 is often used for transcriptional regulation analysis in birds and is an ideal cell model for luciferase reporter gene assays [28–31]. ICP1 and DF-1 cells were cultured in Dulbecco's modified Eagle's medium (DMEM)/F12 and high-glucose DMEM (Gibco, Carlsbad, USA) supplemented with 10% fetal bovine serum (Biological Industries, Kibbutz Beit-Haemek, Israel) and 1% penicillin-streptomycin solution (Beyotime, Shanghai, China), respectively, at 37°C in the presence of 5% CO_2.

Plasmid construction

The overexpression plasmid pCMV-Myc-KLF7 was constructed as described in our previous report [4]. To determine the core region of the CDKN3 promoter, four fragments [nucleotides (nt) –1912/–7, –758/–7, –450/–7, and –160/–7] were amplified using specific primers containing the KpnI and HindIII restriction sites. The PCR products were cloned into the pGL3-Basic vector (Promega, Madison, USA) using a ClonExpress Entry One Step Cloning kit (Vazyme, Nanjing, China). Through DNA synthesis (Genewiz, Suzhou, China), the four putative KLF7-binding sites (nt –137/–128, –87/–79, –72/–64, –56/–47) were specifically deleted in the context of pGL3-CDKN3 (nt –160/–7), and the resultant reporter plasmids were designated as pGL3-CDKN3-DM1, pGL3-CDKN3-DM2, pGL3-CDKN3-DM3, and pGL3-CDKN3-DM4. The full-length coding region of chicken CDKN3 (accession number: NM_001252162.1) was amplified by RT-PCR and cloned into the empty vector pCMV-HA (Clontech, San Francisco, USA) to construct the overexpression plasmid pCMV-HA-CDKN3. All primers used are listed in Table 1.

Three interference fragments, si-CDKN3-1, si-CDKN3-2, si-CDKN3-3, and si-NC, were designed according to the CDKN3 coding sequence and were synthesized by Hanbio Biotechnology (Shanghai, China). The sequences are listed in Table 2.

Cell transfection

When the cell density reached 60%–70%, plasmids or constructs were transfected into the cells using Invitrogen Lipofectamine 2000 reagent (Invitrogen, Carlsbad, USA). Forty-eight hours after transfection, the cells were harvested and immediately subjected to total RNA or protein isolation. Each experiment was repeated three times independently.

Dual-luciferase reporter assay

Dual-luciferase reporter assays were performed using DF-1 and ICP1 cells. To characterize the CDKN3 promoter, cells were transfected with pGL3-CDKN3 or pGL3-Basic. To analyze the effect of KLF7 overexpression on CDKN3 promoter activity, cells were co-transfected with pGL3-CDKN3 and pCMV-Myc-KLF7. The cells were lysed, and promoter activities were assessed using a Dual-Luciferase Assay System (Promega) according to the manufacturer's instructions. The transfection efficiency was normalized to that of the Renilla luciferase vector (pRL-TK). The dual-luciferase reporter assay was performed in three independent experiments with three replicates each.

RNA isolation and RT-qPCR

Total RNA was extracted from ICP1 cells using RNAiso Plus (TaKaRa, Dalian, China) and was reverse-transcribed to cDNA using HiScript II Q Select RT SuperMix (Vazyme). qPCRs were run using 10-μL reaction mixtures containing 1 μL of cDNA, 0.2 μL of each primer, and 5 μL of 2× ChamQ SYBR® qPCR Master Mix (without ROX) (Vazyme) according to the manufacturer's instructions. The thermal cycling conditions were 95°C for 10 min and 35 cycles of 95°C for 15 s and 60°C for 30 s. Relative mRNA levels were normalized to that of an endogenous reference gene (NONO) and were calculated using the $2^{-\Delta\Delta Ct}$ method. Three independent experiments with three replicates each were performed. Primer sequences are listed in Table 1.

Western blot analysis

Forty-eight hours after transfection, cells were lysed on ice for total protein extraction. The total protein was quantified using the bicinchoninic acid assay reagent (Beyotime), separated by 10% polyacrylamide gel electrophoresis, and transferred to a polyvinylidene fluoride membrane (Millipore, Boston, USA) following the manufacturer's instructions. After being blocked with 5% skimmed milk (BD Biosciences, Franklin Lakes, USA), the membrane was incubated with the relevant primary antibody at 4°C overnight and then with the secondary antibody (680LT, 680 RD respectively; dilution ratio 1:5000; LI-COR, Lincoln, USA) at room temperature for 1 h and then scanned using a two-color infrared fluorescence imaging system (Odyssey; LI-COR). After extensive wash with western primary and secondary antibody removal solution (Beyotime), the membranes were hybridized with anti-β-actin antibody (AF0003; 1:1000; Beyotime) as an internal reference. The primary antibodies used were as follows: anti-HA (#3724; 1:1000; CST, Beverly, USA), anti-Myc (AM926; 1:1000; Beyotime), anti-KLF7 (6334-1; 1:200; Abmart, Shanghai, China), anti-Akt (AA326, 1:1000; Beyotime), anti-pAkt-Ser473 (AA329; 1:1000; Beyotime), and anti-pAkt-Thr308 (AA331; 1:1000; Beyotime). Three independent experiments with three replicates each were conducted.

Table 1. Sequences of primers used in this study

Gene	Primer sequence (5′→3′)	GenBank accession number
CDKN3 −1912/−7	F: atttctctatcgataggtaccTAAGGCAATCACAGCACAA	NC_052536.1
	R: cagtaccggaatgccaagcttGGCTGCGGATGGAGAAGA	
CDKN3 −758/−7	F: atttctctatcgataggtaccCCGGAACGAAAGGCTGAG	NC_052536.1
	R: cagtaccggaatgccaagcttGGCTGCGGATGGAGAAGA	
CDKN3 −450/−7	F: atttctctatcgataggtaccCAGTGCTCCTCATCCCA	NC_052536.1
	R: cagtaccggaatgccaagcttGGCTGCGGATGGAGAAGA	
CDKN3 −160/−7	F: atttctctatcgataggtaccCTCGACCAATGAGATGCG	NC_052536.1
	R: cagtaccggaatgccaagcttGGCTGCGGATGGAGAAGA	
CDKN3	F: tggccatggaggcccgaattcTGCACGTAGCCGGCTTTGACTC	NM_001252162.1
	R: gcggccgcggtacctcgagTGCAGCACGAGTTCACCGTGA	
RT-qPCR CDKN3	F: TGTCCTGGCTCCCTCTGTC	NM_001252162.1
	R: CATCCTTAAACCTGCAACCC	
RT-qPCR CDKN1A	F: CCCAGGGATGGTGTCG	NM_204396.1
	R: GGGCTTATCGTGGACAACT	
RT-qPCR CDKN1B	F: CGCTTCTCAGGGAATCTCA	NM_204256.2
	R: GAAACCTCCTCTTCTGTTGTG	
RT-qPCR Ki-67	F: AGGTCCGTTCCCTCGTT	XM_422088.5
	R: CATTGTCGTCTGGGTCATC	
RT-qPCR PCNA	F: GTGCTGGGACCTGGGTT	NM_204170.2
	R: CGTATCCGCATTGTCTTCT	
RT-qPCR Cyclin D1	F: AGAAGTGCGAAGAGGAAGT	NM_205381.1
	R: TGATGGAGTTGTCGGTGTA	
RT-qPCR Cyclin E	F: TTTGCTATGGCTATAAGGG	NM_001031358.1
	R: TGTGGTGGCGTAAGGA	
RT-qPCR NONO	F: AGAAGCAGCAGCAAGAAC	NM_001031532.1
	R: TCCTCCATCCTCCTCAGT	

Table 2. siRNAs used in this study

Name	Sequence (5′→3′)
si-CDKN3-1	F: AGACAAUUAUCCACUGUUAdTdT
	R: UAACAGUGGAUAAUUGUCUdTdT
si-CDKN3-2	F: GUUUGUGCUUUGUACCAAAdTdT
	R: UUUGGUACAAAGCACAAACdTdT
si-CDKN3-3	F: CGGAUGUAGUGACACCUCAdTdT
	R: UGAGGUGUCACUACAUCCGdTdT
si-NC	F: UUCUCCGAACGUGUCACGUdTdT
	R: ACGUGACACGUUCGGAGAAdTdT

Cell viability assay

Cell viability was assessed using the Cell Counting Kit-8 (CCK-8; Dojindo, Shanghai, China). ICP1 cells were cultured in 96-well plates and transfected with pCMV-HA-CDKN3 or si-CDKN3 to up- or downregulate CDKN3 expression, respectively. Six hours after transfection, which was considered time point 0, the cells were incubated with 10 μL of CCK-8 in the dark for 2 h, after which the absorbance at 450 nm was measured using a Model 680 Microplate Reader (Bio-Rad, Hercules, USA). Data were recorded at 0, 12, 24, 48, and 72 h. Three independent experiments with three replicates each were conducted.

Cell proliferation assay

Cell proliferation was assessed using the 5-ethynyl-2′-deoxyuridine (EdU). ICP1 cells seeded in 6-well plates were cultured to 70%–80% density and then transfected with the relevant siRNAs or overexpression vector. Forty-eight hours after transfection, the cells were fixed and stained using the BeyoClick EdU-488 Cell Proliferation Assay kit (Beyotime). An inverted fluorescence microscope (Olympus, Beijing, China) was used to capture images of cells in three randomly selected fields, and ImageJ software was used to count EdU-stained cells. The experiment was repeated three times independently.

Cell cycle analysis by flow cytometry

Flow cytometry was used to detect the proportion of cells in each cell cycle phase using the Cell Cycle and Apoptosis Detection kit (Beyotime) according to the manufacturer's instructions. ICP1 cells were transfected with plasmid DNA (pCMV-HA-CDKN3, pCMV-HA) or siRNA (si-CDKN3 or si-NC). Forty-eight hours later, the cells were harvested and fixed in 70% ethanol at −20°C overnight. After removal of the fixation medium by centrifugation at 266 g, 500 μg of propidium iodide staining solution (Beyotime) was added to the pelleted cells. The mixture was incubated at 37°C for 30 min. Red fluorescence was observed with a flow cytometer (Beckman Coulter, Brea, USA) at an excitation wavelength of 488 nm.

Statistical and bioinformatics analyses

Transcription factor-binding sites were predicted using the JASPAR [32] online database. Correlation was calculated using Pearson's product-moment correlation. Statistical analyses were performed using the SPSS package (IBM SPSS Statistics for Windows, v.22.0; IBM, Armonk, USA). Data are shown as the mean ± standard deviation (SD). Means of two groups were compared using two-way Student's *t* test. *P* < 0.05 was considered statistically significant.

Results

KLF7 and *CDKN3* expression are positively correlated in chicken adipose tissue

To explore whether KLF7 is functionally associated with *CDKN3* in chicken preadipocytes, we first detected *KLF7* and *CDKN3* expressions in abdominal adipose tissues collected from AA commercial broilers 1–7 weeks of age (Figure 1) and statistically analyzed the correlation. The results showed that *CDKN3* expression significantly declined from 1 to 6 weeks of age (*P* < 0.05; Figure 1), whereas *KLF7* expression tended to decline from 1 to 6 weeks of age (*P* > 0.05; Figure 1). Pearson's correlation analysis showed a significant positive correlation between *KLF7* expression and *CDKN3* expression at 1–7 weeks of age (*r* = 0.734, *P* = 0.000, *n* = 21).
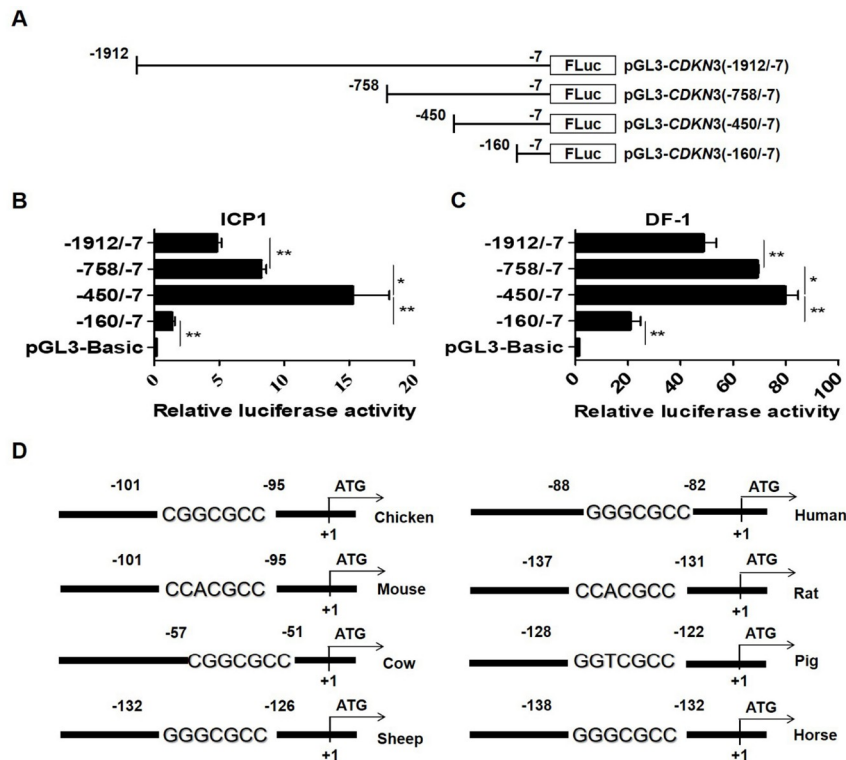
Characterization of the chicken *CDKN3* promoter

To characterize the *CDKN3* promoter, we constructed four 5′-truncated mutant luciferase reporter gene plasmids, pGL3-*CDKN3* (nt –1912/–7), pGL3-*CDKN3* (nt –758/–7), pGL3-*CDKN3* (nt –450/–7), and pGL3-*CDKN3* (nt –160/–7) (Figure 2A), and transfected them into ICP1 and DF-1 cells. The luciferase activity assay results showed that all constructs generated stronger promoter activity than the empty pGL3-Basic vector (*P* < 0.05; Figure 2B,C). Notably, pGL3-*CDKN3* (nt –160/–7) retained basal promoter activity when compared with pGL3-Basic (*P* < 0.01; Figure 2C,D). Bioinformatics analysis using the Promoter Inspector server predicted that the nt –160/–7 region contained an upstream core promoter element CGGCGCC (nt –101/–95) (Figure 2D). We also found core promoter
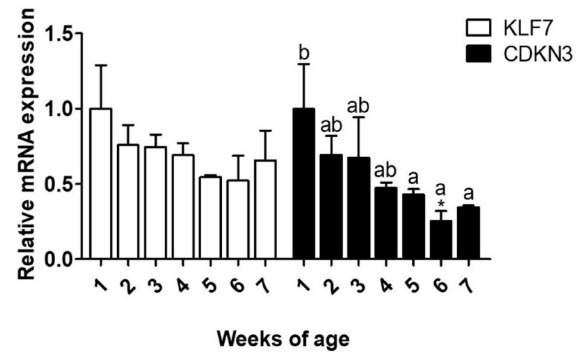
Figure 1. *KLF7* and *CDKN3* expressions in abdominal adipose tissues of AA commercial broilers of 1–7 weeks of age   Gene expression was determined by RT-qPCR. Data are shown as the mean ± SD (*n* = 21). **P* < 0.05, Student's *t* test. The different letters above the columns indicate significant differences among groups (Duncan's multiple test, *P* < 0.05).

Figure 2. Characterization of the chicken *CDKN3* promoter   (A) Schematic diagram of the *CDKN3* reporter constructs used in this study. (B,C) Analysis of *CDKN3* promoter activity. Luciferase reporter vectors were transfected into ICP1 (B) or DF-1 (C) cells with pRL-TK (transfection ratio 100:1). Relative luciferase activity was calculated as the ratio of firefly to *Renilla* luciferase activity. (D) The CGGCGCC core promoter element of chicken *CDKN3* is located at nt –101/–95 (the ATG codon, the transcription start site of *CDKN3*, is considered position + 1). Promoter core elements (G/C)(G/C)(G/A)CGCC of *CDKN3* in various other species are shown for comparison. Data are shown as the mean ± SD. **P* < 0.05, ***P* < 0.01, Student's *t* test.

elements (G/C)(G/C)(G/A)CGCC in this region of human, mouse, rat, pig, cow, sheep, and horse *CDKN3* (Figure 2D). These results indicated that nt –160/–7 bp is the minimum promoter region of chicken *CDKN3*.
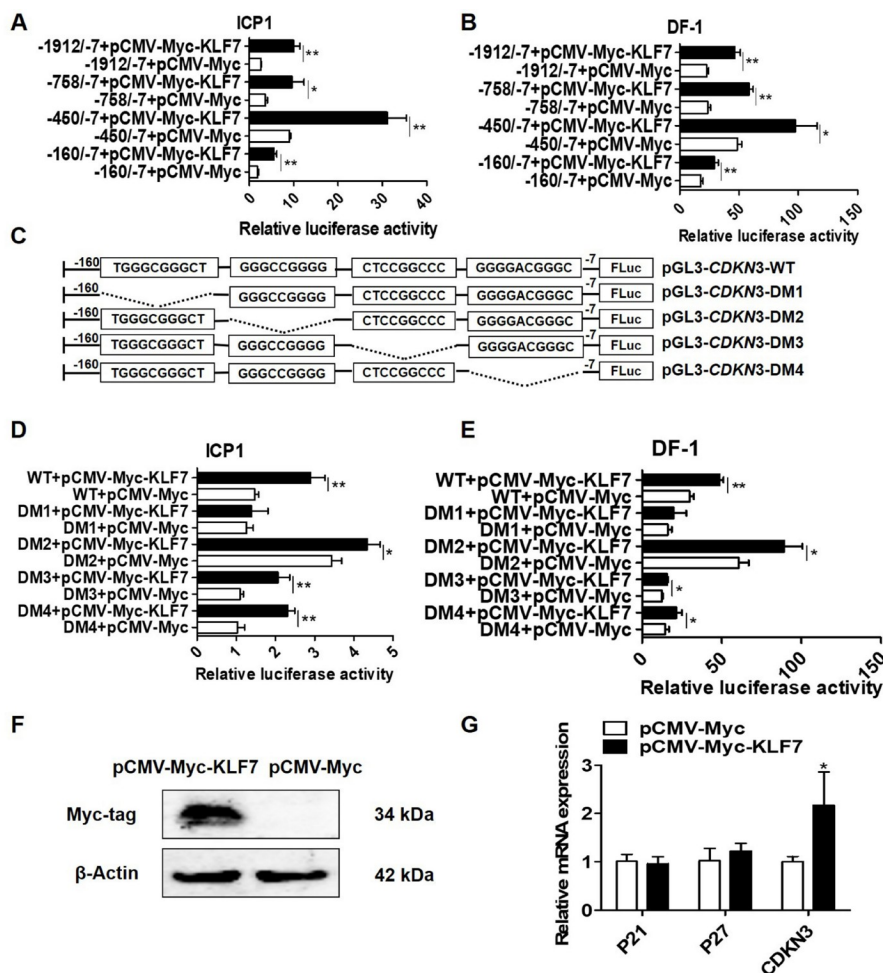
KLF7 promotes *CDKN3* transcription

To determine the effect of KLF7 on *CDKN3* promoter activity, four 5′-terminal deletion firefly luciferase reporter gene constructs were co-transfected with pCMV-Myc-KLF7 into ICP1 and DF-1 cells. Luciferase activity assay results showed that KLF7 overexpression significantly enhanced the promoter activity of all four reporter gene constructs, including the one containing the shortest *CDKN3* promoter fragment (–160/–7) ($P < 0.01$; Figure 3A,B), suggesting that the minimal promoter, *CDKN3* nt –160/–7, has a KLF7-binding site.

Next, we determined the binding site of KLF7 in the *CDKN3* promoter. We attempted to find the KLF7-binding motif revealed by our previous ChIP-seq analysis (data not shown); however, we could not find it. Therefore, we predicted KLF7-binding sites in the *CDKN3* promoter using the Jaspar online database [32] and found

four potential KLF7-binding sites in this region (Figure 3C). We deleted the four potential binding sites based on the pGL3-*CDKN3* (nt –160/–7) promoter construct. The deletion reporter constructs, designated as pGL3-*CDKN3*-DM1, pGL3-*CDKN3*-DM2, pGL3-*CDKN3*-DM3, and pGL3-*CDKN3*-DM4, were co-transfected with pCMV-Myc-KLF7 into ICP1 and DF-1 cells. Luciferase activity assay results showed that deletion of the DM1 site TGGGCGGGCT (nt –137/–128) nearly completely abolished the effect of KLF7 on the promoter activity of pGL3-*CDKN3* (nt –160/–7) ($P < 0.05$), whereas the other three deletions had no apparent effect ($P > 0.05$; Figure 3D, E). These results indicated that the binding site TGGGCGGGCT (nt –137/–128) is required for KLF7 to exert activity on the *CDKN3* promoter. In addition, we also statistically compared the fold-induction of the different deletion mutants to the wild-type. The results showed that the induction of DM2 and DM3 was significantly reduced in ICP1 and DF-1 cells, respectively ($P < 0.05$), indicating that these two sites also contribute to the response.

Previous studies in mammals have demonstrated that KLF7

Figure 3. KLF7 facilitates *CDKN3* transcription (A,B) Reporter gene assays of the effect of KLF7 overexpression on *CDKN3* promoter activity in ICP1 (A) and DF-1 (B) cells. Relative luciferase activity was calculated as the ratio of firefly to *Renilla* luciferase activity. (C) Schematic representation of the binding site-deletion constructs. Each of the four potential core sequences is depicted in a box. A dashed line indicates core sequence deletion. (D, E) Analysis of KLF7 binding to the *CDKN3* promoter using a reporter gene assay. The wild-type reporter pGL3-*CDKN3* (WT) or the DM deletion vectors and pCMV-Myc-KLF7 were co-transfected into ICP1 (D) and DF-1 (E) cells. Relative luciferase activity was calculated as the ratio of firefly to *Renilla* luciferase activity. (F) Myc protein expression levels. (G) *P21*, *P27*, and *CDKN3* transcript levels in ICP1 cells. Data are shown as the mean ± SD. *$P < 0.05$, **$P < 0.01$, Student's *t* test.

drives neurogenesis by regulating the expression of *P21* (also named *CDKN1A*) [33] and *P27* (also named *CDKN1B*) [34], two other members of the CIP/KIP family. To determine whether KLF7 also acts on *P21* and *P27* in chicken preadipocytes, pCMV-Myc-KLF7 and pCMV-Myc were transfected into ICP1 cells, and Myc expression levels were detected by western blot analysis to confirm KLF7 overexpression (Figure 3F). RT-qPCR results showed that overexpression of KLF7 increased the endogenous expression of *CDKN3* ($P < 0.05$) but did not affect the expressions of *P21* and *P27* ($P > 0.05$; Figure 3G).

CDKN3 upregulates preadipocyte proliferation

To detect whether *CDKN3* is involved in chicken preadipocyte proliferation, *CDKN3* expression was detected during the proliferation of ICP1 cells. CCK-8-based cell viability assay showed that ICP1 cells gradually increased in number from 0 h to 72 h (Figure 4A), indicating that the cells were proliferating normally. RT-qPCR analysis showed that *CDKN3* was expressed during this process (Figure 4B), suggesting that *CDKN3* plays a role in ICP1 cell proliferation.

To explore the functions of *CDKN3* in chicken preadipocyte proliferation, we performed overexpression and interference assays. The effects of *CDKN3* overexpression (Figure 4C,D) and interference (Figure 5A) in ICP1 cells were analyzed by western blot analysis and RT-qPCR. *CDKN3* overexpression promoted the expressions of the proliferation markers *Ki-67*, *PCNA*, and *Cyclin E* ($P < 0.05$; Figure 4E), whereas *CDKN3* interference significantly suppressed the transcript levels of these markers ($P < 0.05$; Figure 5B). Moreover, CCK-8 and EdU assay results showed that *CDKN3* overexpression significantly enhanced ICP1 cell proliferation ($P < 0.05$; Figure 4F–H), whereas proliferation was significantly reduced after *CDKN3* interference ($P < 0.05$; Figure 5C–E).

To determine the role of *CDKN3* in the cell cycle, the percentage of ICP1 cells in each phase of the cell cycle was assessed by flow cytometry. Overexpression of *CDKN3* significantly reduced the number of cells in the G0/G1 phase ($P < 0.05$; Figure 4I,J), whereas *CDKN3* interference markedly decreased the number of cells remaining in the S phase ($P < 0.05$; Figure 5F,G). These results implied that *CDKN3* promotes preadipocyte proliferation by driving the G1/S transition.

## KLF7 activates the Akt signaling pathway by upregulating *CDKN3* expression

KLF7 is a positive regulator of chicken preadipocyte proliferation [4]. We showed that *CDKN3* promoted preadipocyte proliferation (Figures 4 and 5) and that *CDKN3* transcription was enhanced by KLF7 (Figure 3). Therefore, we further investigated whether KLF7 promotes preadipocyte proliferation by upregulating *CDKN3* expression by EdU assay. The proliferation of cells transfected with pCMV-Myc-KLF7 was significantly higher than that of cells transfected with pCMV-Myc ($P < 0.01$; Figure 6A,B), indicating that KLF7 overexpression promotes preadipocyte proliferation. The proliferation of cells transfected with si-*CDKN3* was lower than that of cells in the NC group ($P < 0.05$; Figure 6A,B), indicating that *CDKN3* inference reduces chicken preadipocyte proliferation. There were no remarkable differences in proliferation between the si-NC group and KLF7 overexpression + si-*CDKN3* group ($P > 0.05$; Figure 6A,B). These results suggested that KLF7 promotes proliferation by upregulating *CDKN3* expression.

As the Akt signaling pathway plays a key role in cell cycle regulation [35] and *CDKN3* reportedly activates Akt phosphorylation in cancer cells [36–38], we investigated whether KLF7 activates the Akt pathway by upregulating *CDKN3* in ICP1 cells. Western blot analysis results showed that, compared with the Myc + si-*CDKN3* and Myc + si-NC groups, the KLF7 + si-*CDKN3* and KLF7 + si-NC groups showed significantly higher KLF7 expression ($P < 0.05$), which demonstrated that KLF7 was successfully overexpressed. Western blot analysis results also showed that KLF7 overexpression significantly enhanced the levels of pAkt^{Thr308} ($P < 0.05$) and pAkt^{Ser473} ($P < 0.05$) compared with those in the control group, suggesting that KLF7 promotes proliferation by enhancing Akt signaling activation in chicken preadipocytes. The levels of pAkt^{Thr308} ($P < 0.01$) and pAkt^{Ser473} ($P < 0.01$) were lower in the si-*CDKN3* group than in the si-NC group, implying that *CDKN3* knockdown repressed Akt signaling activation. There were no significant differences in pAkt^{Thr308} and pAkt^{Ser473} levels between the si-NC and KLF7 + si-*CDKN3* groups ($P > 0.05$; Figure 6C,D). Together, the present findings revealed that KLF7 overexpression facilitates Akt pathway activation by upregulating *CDKN3* expression.

Discussion

KLF7 is a positive regulator of chicken preadipocyte proliferation [4]; however, the underlying mechanism remains poorly understood. The current study confirmed that KLF7 overexpression promoted preadipocyte proliferation (Figure 6A,B) and showed that this promotion was achieved via the Akt signaling pathway (Figure 6C,D). Furthermore, we found that KLF7 upregulated *CDKN3* promoter activity, and the binding site TGGGCGGGCT (−137/−128 nt; DM1) is required for KLF7 to exert activity on the *CDKN3* promoter (Figure 3D, E). In addition, KLF7 overexpression promoted the endogenous expression of *CDKN3* (Figure 3G). Based on our previous ChIP-qPCR and ChIP-seq-based finding that KLF7 can bind to the promoter region of *CDKN3*, we demonstrated that DM1 likely mediates KLF7 binding to the *CDKN3* promoter to drive *CDKN3* transcription. However, as we did not assess combined binding site mutations and the fold-induction of DM2 and DM3 was significantly reduced compared with the wild-type, we cannot assert that DM1 is the only binding site. Moreover, deletion of the binding site may have led to the formation of new binding sites that affected *CDKN3* promoter activity. Despite these limitations, our results still revealed the mechanism by which KLF7 facilitates preadipocyte proliferation.

P21 (also named CDKN1A) [33] and P27 (also named CDKN1B) [34] are CIP/KIP family members [39,40]. P21 can bind to CDK to inhibit its interaction with substrates such as Rb family members, ultimately repressing G1/S progression [41]. P27 also inhibits CDK activity, thus blocking the G1/S transition and cell cycle progression [42]. KLF7 reportedly targets *P21* and *P27* in various mammalian cells. In nerve cells, KLF7 promotes *P21* and *P27* expressions to drive axon outgrowth [33,34]. KLF7 also maintains muscle stem satellite cells in quiescence and drives cell cycle exit by acting on *P21* [43]. The role of KLF7 in preadipocyte proliferation in mice remains unclear. Interestingly, unlike murine *KLF7*, chicken *KLF7* upregulated *CDKN3* expression but had no effect on *P21* and *P27* in preadipocytes (Figure 3G), implying that the molecular mechanisms of KLF7 in preadipocytes differ between birds and mammals. In the present study, we performed gene expression analysis of chicken *CDKN3*, but due to the lack of available chicken antibodies, we did
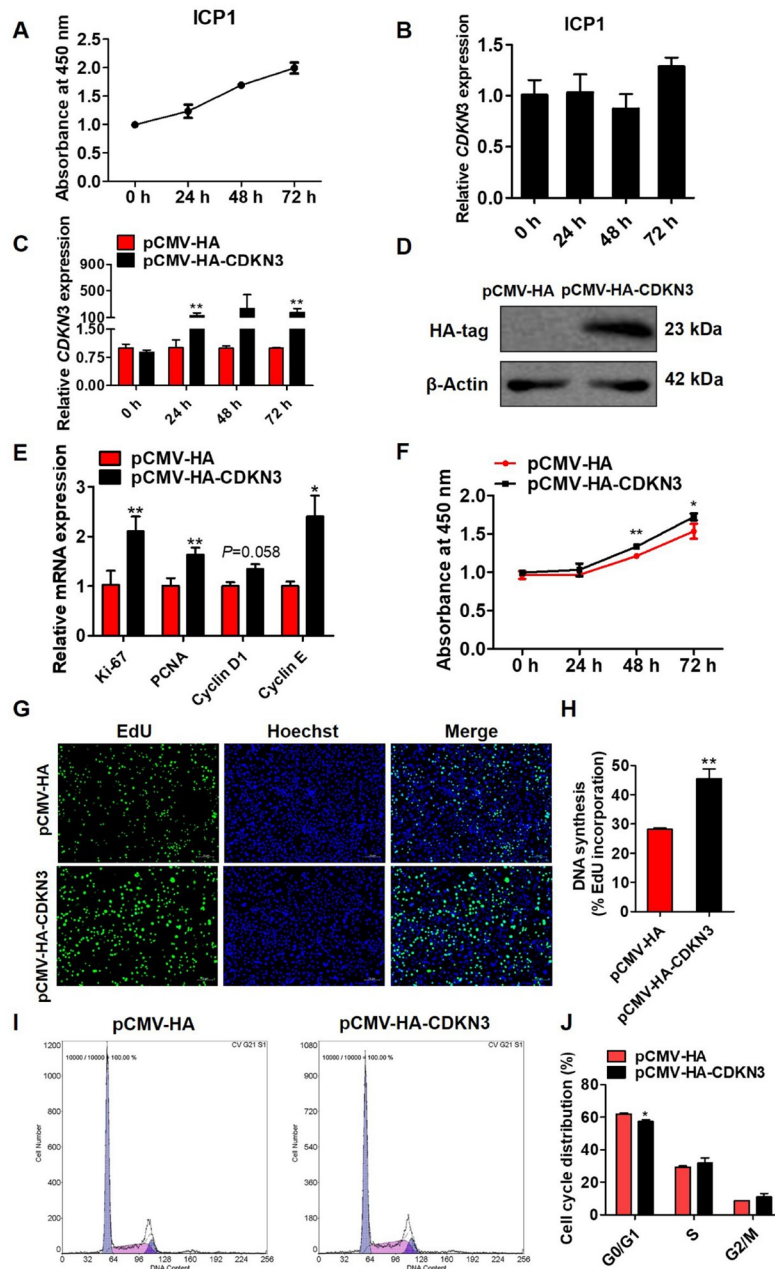
Figure 4. CDKN3 overexpression upregulates ICP1 cell proliferation (A) ICP1 cell viability was determined by CCK-8 assay. The OD_{450} value represents the proliferation capacity determined in three independent experiments. (B) RT-qPCR was used to detect *CDKN3* expression during proliferation. (C) RT-qPCR was used to verify the overexpression of pCMV-HA-CDKN3 in ICP1 cells at 0, 24, 48, and 72 h after transfection. (D) Western blot analysis was used to verify the effect of pCMV-HA-CDKN3 overexpression on ICP1 cells 48 h after transfection. Western blot analysis was repeated three times, and representative results are shown. (E) Transcript levels of *Ki-67*, *PCNA*, *Cyclin D1*, and *Cyclin E* were detected by RT-qPCR at 48 h post transfection. (F) The CCK-8 assay was used to detect the effect of CDKN3 overexpression on ICP1 cell proliferation. The line chart shows light absorption at 450 nm. (G,H) Proliferation of ICP1 cells transfected with pCMV-CDKN3 as assessed based on EdU incorporation (green fluorescence). (I,J) Effect of CDKN3 overexpression on the ICP1 cell cycle in ICP1 cells as measured by flow cytometry. Data are shown as the mean ± SD. *$P < 0.05$, **$P < 0.01$, Student's *t* test.

not perform protein expression analysis, and it is worth performing protein expression analysis. In addition, we did not test the effects of *KLF7* knockdown. For some reason, the chemically synthesized KLF7 siRNAs did not work. Thus, it would be worth further exploring the functions of chicken KLF7 and *CDKN3 in vivo* or *in vitro* using CRISPR/Cas9 assays.

Preadipocyte proliferation is controlled by a complex network of transcription factors [4–6]. For example, BMP4 upregulates the proliferation of ICP1 cells by promoting the G1/S transition [44], whereas ALDH1A1 is a negative regulator of preadipocyte proliferation and inhibits the G1/S transition [45]. Many other factors, such as PPARγ [46], RB1 [47], HOPX [48], and TCF21 [49], also play negative regulatory roles in preadipocyte proliferation. In the present study, we showed for the first time that *CDKN3*
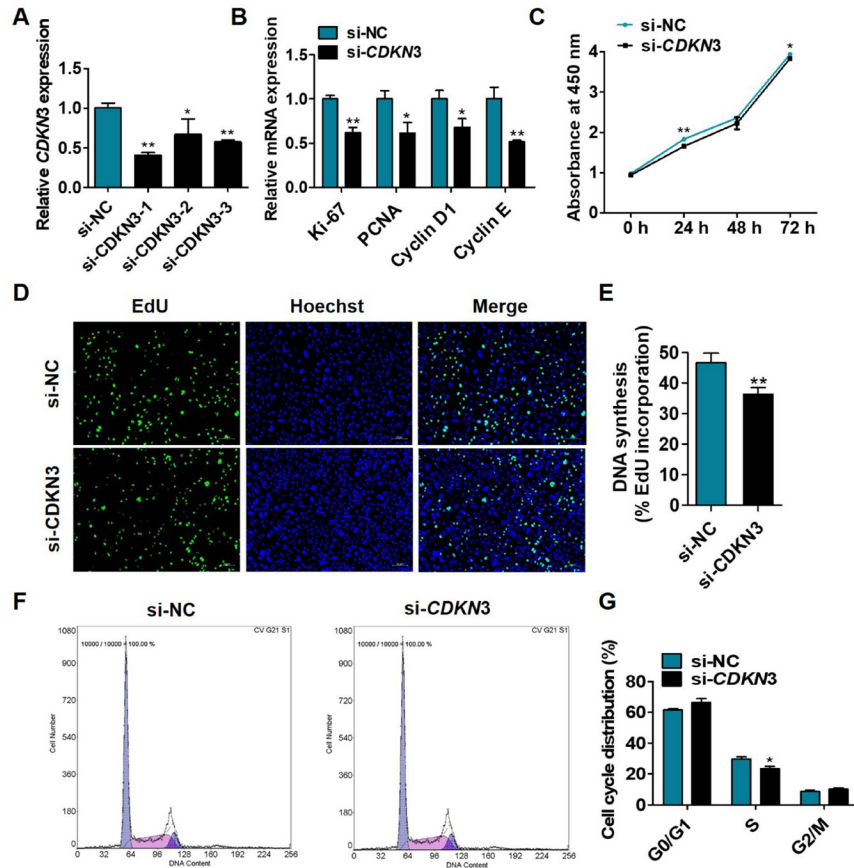
Figure 5. CDKN3 interference reduces ICP1 cell proliferation (A) Effects of CDKN3 interference in ICP1 cells as detected by RT-qPCR 48 h after transfection. (B) RT-qPCR was used to detect the effect of CDKN3 interference on the expressions of the cell proliferation marker genes *Ki-67*, *PCNA*, *Cyclin D1*, and *Cyclin E*. (C) The CCK-8 assay was used to detect ICP1 cell viability upon CDKN3 interference. (D,E) Proliferation of si-*CDKN3*-transfected ICP1 cells as assessed based on EdU incorporation (green fluorescence). (F,G) Effect of CDKN3 interference on the cell cycle of ICP1 cells was assessed by flow cytometry. Data are shown as the mean ± SD. *$P < 0.05$, **$P < 0.01$, Student's *t* test.

promotes preadipocyte proliferation, as evidenced and validated by three independent methods (CCK-8 and EdU assays and flow cytometry; Figures 4 and 5) that were repeated at least three times independently. Our results extend our knowledge of the molecular mechanism underlying chicken preadipocyte proliferation. Because the siRNA (si-*CDKN3*) we used acted for a short time or may have been at the limit of transfection efficiency, the CCK-8 results showed a small difference. It may be worth further exploring the functions of *CDKN3* using the CRISPR/Cas9 assay or by constructing lentiviral vectors.

CDKN3, also known as CDI1, CIP2, KAP, or KAP1, was first discovered as a binding protein of cyclin-dependent kinase 2 (CDK2). Studies have shown that *CDKN3* promotes the proliferation of breast [50] and prostate [51] cancer cells. Consistent with these findings, we found that *CDKN3* induced preadipocyte proliferation by driving the G1/S transition and inducing the expression of cyclin E, a G1/S progression promoter. Interestingly, our data contradicted a previous finding that *CDKN3* inhibits the G1/S transition by dephosphorylating CDC2^{Thr161} in brain glioma cells [52]. This discrepancy suggests that *CDKN3* drives or represses cell proliferation in a cell- or context-specific manner.

The Akt/mTOR pathway plays critical roles in regulating the cell cycle and apoptosis [53]. Several studies have reported that Akt pathway activation promotes preadipocyte proliferation [54,55].

We found that *CDKN3* increased Akt pathway activation in preadipocytes (Figure 6C,D) and promoted preadipocyte proliferation (Figures 4–6). Moreover, KLF7 induced Akt signaling activation by targeting *CDKN3* (Figure 7). *CDKN3* promotes the ubiquitination and subsequent phosphorylation of Akt by preventing the interaction between SKP2 and CDK2 via the dephosphorylation of CDK2 [37]. The Akt pathway also has important functions in preadipocyte differentiation. Studies have shown that Akt pathway activation promotes the expressions of PPARγ and C/EBPα, two key regulators of differentiation, thus accelerating preadipocyte differentiation [56–58]. Notably, KLF7 downregulates preadipocyte differentiation [4]. However, our results indicated that both KLF7 and *CDKN3* accelerated Akt pathway activation in preadipocytes. Altogether, these data suggested that KLF7 boosts preadipocyte proliferation by promoting Akt signaling via targeting *CDKN3*, whereas in preadipocyte differentiation, KLF7 may not play an inhibitory role via *CDKN3* and Akt pathway activation.

Chicken is an ideal model species for studying adipogenesis and adipose biology in view of its natural hyperglycemia, insulin resistance, hepatic fatty acid synthesis, and reproductive system [22]. In particular, their high glycemia and low sensitivity to exogenous insulin (particularly in adipose tissues) make them a relevant model for studies on human obesity, insulin resistance, and type 2 diabetes [20,21,59]. In this study, we showed that
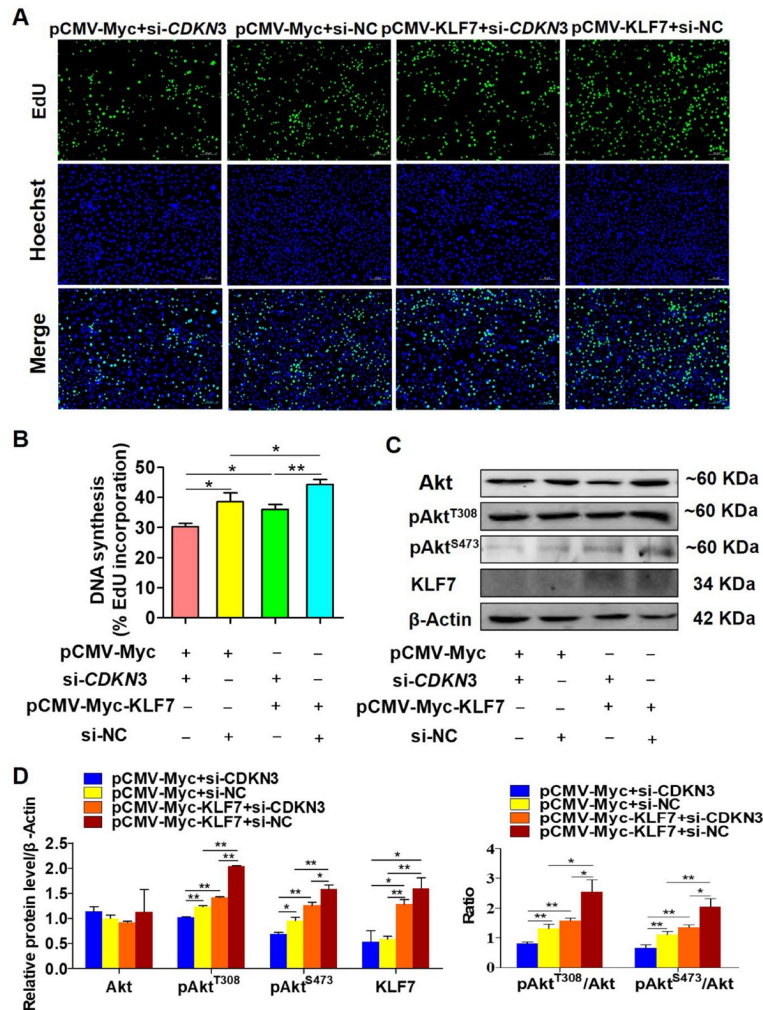
Figure 6. KLF7 activates the Akt signaling pathway via CDKN3 (A,B) Forty-eight hours after transfection, the proliferation of ICP1 cells transfected with pCMV-Myc-KLF7 and si-*CDKN3* was assessed based on EdU incorporation (green fluorescence). (C,D) Western blot analysis was used to detect the effects of KLF7 overexpression and *CDKN3* interference on Akt, pAkt^{T308}, and pAkt^{S473} levels. The analysis was repeated three times independently, and representative results are shown. Data are shown as the mean $\pm$ SD. *$P < 0.05$, **$P < 0.01$, Student's *t* test.

KLF7 increased the number of ICP1 cells by promoting *CDKN3* transcription. These results provide insights into the molecular regulatory network of preadipocyte proliferation and contribute to understanding human adipogenesis and obesity, which is of great significance given the high prevalence of obesity nowadays. In addition, our findings suggest that *CDKN3* may be a potential therapeutic target for human obesity and obesity-related diseases.

In conclusion, we showed for the first time that *CDKN3* is a target gene of the transcription factor KLF7 in preadipocytes. *CDKN3* promotes preadipocyte proliferation by driving the G1/S transition. By upregulating *CDKN3*, KLF7 accelerates Akt signaling pathway activation, thereby facilitating preadipocyte proliferation in chickens.

Acknowledgement

Funding

References

1. Tobore TO. Towards a comprehensive theory of obesity and a healthy diet: the causal role of oxidative stress in food addiction and obesity. *Behav Brain Res* 2020, 384: 112560

2. Tang QQ, Lane MD. Adipogenesis: from stem cell to adipocyte. *Annu Rev Biochem* 2012, 81: 715–736

3. Tontonoz P, Spiegelman BM. Fat and beyond: the diverse biology of PPARγ. *Annu Rev Biochem* 2008, 77: 289–312

4. Zhang Z, Wang H, Sun Y, Li H, Wang N. Klf7 modulates the differentiation and proliferation of chicken preadipocyte. *Acta Biochim Biophys Sin* 2013, 45: 280–288
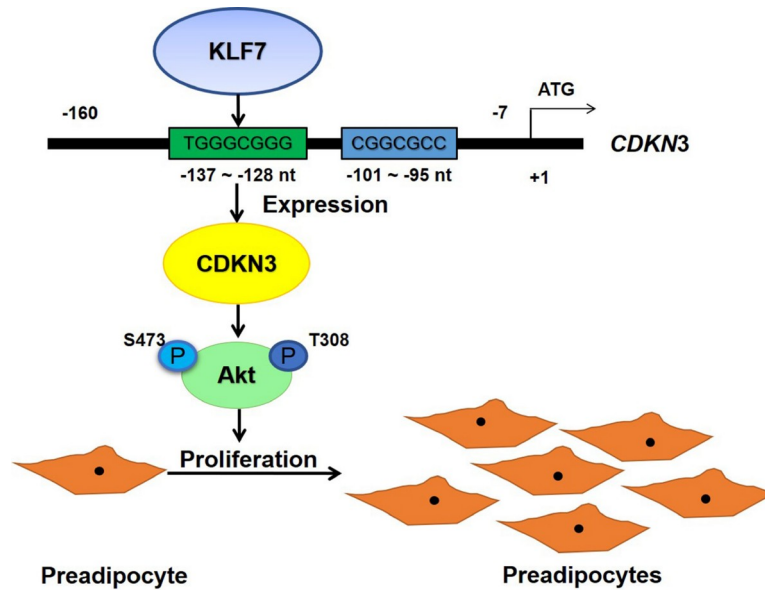
Figure 7. KLF7 promotes the proliferation of preadipocytes via CDKN3-mediated regulation of Akt phosphorylation The transcription factor KLF7 can directly bind to the promoter region of *CDKN3* to promote *CDKN3* expression. CDKN3 drives the G1/S transition, thus promoting ICP1 cell proliferation by activating the Akt pathway via Ser and Thr phosphorylation.

5. Xiao C, Jin HG, Zhang LC, Liu JQ, He M, Ma HH, Yu YS, *et al.* Effects of SPARCL1 on the proliferation and differentiation of sheep preadipocytes. *Adipocyte* 2021, 10: 658–669

6. Zhang W, Chen Q, Xu L, Cai J, Zhang J. The potential role of PSMA6 in modulating fat deposition in pigs by promoting preadipocyte proliferation and differentiation. *Gene* 2021, 769: 145228

7. Mortensen SB, Jensen CH, Schneider M, Thomassen M, Kruse TA, Laborda J, Sheikh SP, *et al.* Membrane-tethered delta-like 1 homolog (DLK1) restricts adipose tissue size by inhibiting preadipocyte proliferation. *Diabetes* 2012, 61: 2814–2822

8. Wang W, Cheng M, Qiao S, Wang Y, Li H, Wang N. Gga-miR-21 inhibits chicken pre-adipocyte proliferation in part by down-regulating Kruppel-like factor 5. *Poultry Sci* 2017, 96: 200–210

9. Zhang L, Zhang D, Qin ZY, Li J, Shen ZY. The role and possible mechanism of long noncoding RNA PVT1 in modulating 3T3-L1 preadipocyte proliferation and differentiation. *IUBMB Life* 2020, 72: 1460–1467

10. Rane MJ, Zhao Y, Cai L. Krüppel-like factors (KLFs) in renal physiology and disease. *EBioMedicine* 2019, 40: 743–750

11. Karp JE, Rassool FV. KLFs and ATRA-induced differentiation: new pathways for exploitation. *Leukemia Res* 2011, 35: 846–847

12. Zhang ZW, Wang ZP, Zhang K, Wang N, Li H. Cloning, tissue expression and polymorphisms of chicken Krüppel-like factor 7 gene. *Anim Sci J* 2013, 84: 535–542

13. Pan CG, Ouyang CB, Sun CL, Li CS, Chen CJ, Chen CX, Sun CY, *et al.* Decreased serum kruppel-like factor 7 level is positively associated with low-density lipoprotein cholesterol level in women with polycystic ovary syndrome. *Clin Lab* 2019, 65

14. Kanazawa A, Kawamura Y, Sekine A, Iida A, Tsunoda T, Kashiwagi A, Tanaka Y, *et al.* Single nucleotide polymorphisms in the gene encoding Krüppel-like factor 7 are associated with type 2 diabetes. *Diabetologia* 2005, 48: 1315–1322

15. Makeeva OA, Sleptsov AA, Kulish EV, Barbarash OL, Mazur AM, Prokhorchuk EB, Chekanov NN, *et al.* Genomic study of cardiovascular continuum comorbidity. *Acta Naturae* 2015, 7: 89–99

16. Vangala RK, Ravindran V, Ghatge M, Shanker J, Arvind P, Bindu H, Shekar M, *et al.* Integrative bioinformatics analysis of genomic and proteomic approaches to understand the transcriptional regulatory program in coronary artery disease pathways. *PLoS ONE* 2013, 8: e57193

17. Kawamura Y, Tanaka Y, Kawamori R, Maeda S. Overexpression of kruppel-like factor 7 regulates adipocytokine gene expressions in human adipocytes and inhibits glucose-induced insulin secretion in pancreatic β-cell line. *Mol Endocrinol* 2006, 20: 844–856

18. Sun Y, Jin Z, Zhang X, Cui T, Zhang W, Shao S, Li H, *et al.* GATA binding protein 3 is a direct target of kruppel-like transcription factor 7 and inhibits chicken adipogenesis. *Front Physiol* 2020, 11: 610

19. Jin Z, Shao SL, Tan M, Li JW, Jia BH, Wang WY, Zhou, Y, *et al.* KLF7 affects development of broiler adipose tissue by inhibiting hypoxia-inducible factor 1 alpha transcription. *Chinese Journal of Biochemistry and Molecular Biology* 2021, 37: 363–371

20. Dupont J, Métayer-Coustard S, Ji B, Ramé C, Gespach C, Voy B, Simon J. Characterization of major elements of insulin signaling cascade in chicken adipose tissue: apparent insulin refractoriness. *Gen Comp Endocrinol* 2012, 176: 86–93

21. Ji B, Ernest B, Gooding JR, Das S, Saxton AM, Simon J, Dupont J, *et al.* Transcriptomic and metabolomic profiling of chicken adipose tissue in response to insulin neutralization and fasting. *BMC Genomics* 2012, 13: 441

22. Mellouk N, Ramé C, Barbe A, Grandhaye J, Froment P, Dupont J. Chicken is a useful model to investigate the role of adipokines in metabolic and reproductive diseases. *Int J Endocrinol* 2018, 2018: 1–19

23. Hannon GJ, Casso D, Beach D. KAP: a dual specificity phosphatase that interactswith cyclin-dependent kinases. *Proc Natl Acad Sci USA* 1994, 91: 1731–1735

24. Wang W, Zhang T, Wu C, Wang S, Wang Y, Li H, Wang N. Immortalization of chicken preadipocytes by retroviral transduction of chicken TERT and TR. *PLoS ONE* 2017, 12: e0177348

25. Himly M, Foster DN, Bottoli I, Iacovoni JS, Vogt PK. The DF-1 chicken fibroblast cell line: transformation induced by diverse oncogenes and cell death resulting from infection by avian leukosis viruses. *Virology* 1998, 248: 295–304

26. Cui T, Xing T, Huang J, Mu F, Jin Y, You X, Chu Y, *et al.* Nuclear respiratory factor 1 negatively regulates the P1 promoter of the peroxisome proliferator-activated receptor-γ gene and inhibits chicken adipogenesis. *Front Physiol* 2018, 9: 1823

27. Guo L, Chao X, Huang W, Li Z, Luan K, Ye M, Zhang S, *et al.* Whole transcriptome analysis reveals a potential regulatory mechanism of lncRNA-FNIP2/miR-24-3p/FNIP2 axis in chicken adipogenesis. *Front Cell Dev Biol* 2021, 9: 653798

28. Bu G, Fan J, Yang M, Lv C, Lin Y, Li J, Meng F, *et al.* Identification of a novel functional corticotropin-releasing hormone (CRH2) in chickens and its roles in stimulating pituitary TSHβ expression and ACTH secretion. *Front Endocrinol* 2019, 10: 595

29. Wang Z, Ouyang H, Chen X, Yu J, Abdalla BA, Chen B, Nie Q. Gga-miR-205a affecting myoblast proliferation and differentiation by targeting CDH11. *Front Genet* 2018, 9: 414

30. Zhang L, Zhu R, Zuo Q, Li D, Lian C, Tang B, Xiao T, *et al.* Activity analysis and preliminary inducer screening of the chicken DAZL gene promoter. *Int J Mol Sci* 2015, 16: 6595–6605

31. Li J, Meng F, Song C, Wang Y, Leung FC. Characterization of chicken visfatin gene: cDNA cloning, tissue distribution, and promoter analysis. *Poultry Sci* 2012, 91: 2885–2894

32. Roy D, Farabaugh KT, Wu J, Charrier A, Smas C, Hatzoglou M, Thirumurugan K, *et al.* Coordinated transcriptional control of adipocyte triglyceride lipase (Atgl) by transcription factors Sp1 and peroxisome proliferator–activated receptor γ (PPARγ) during adipocyte differentiation. *J Biol Chem* 2017, 292: 14827–14835

33. Smaldone S, Laub F, Else C, Dragomir C, Ramirez F. Identification of MoKA, a novel f-box protein that modulates kruppel-like transcription factor 7 activity. *Mol Cell Biol* 2004, 24: 1058–1069

34. Laub F, Lei L, Sumiyoshi H, Kajimura D, Dragomir C, Smaldone S, Puche AC, *et al.* Transcription factor KLF7 is important for neuronal morphogenesis in selected regions of the nervous system. *Mol Cell Biol* 2005, 25: 5699–5711

35. Arcaro A, Guerreiro AS. The phosphoinositide 3-kinase pathway in human cancer: genetic alterations and therapeutic implications. *Curr Genomics* 2007, 8: 271–306

36. Lin WR, Lai MW, Yeh CT. Cyclin-dependent kinase-associated protein phosphatase is overexpressed in alcohol-related hepatocellular carcinoma and influences xenograft tumor growth. *Oncol Rep* 2013, 29: 903–910

37. Li Y, Yang Q, Guan H, Shi B, Ji M, Hou P. ZNF677 suppresses akt phosphorylation and tumorigenesis in thyroid cancer. *Cancer Res* 2018, 78: 5216–5228

38. Liu J, Min L, Zhu S, Guo Q, Li H, Zhang Z, Zhao Y, *et al.* Cyclin-dependent kinase inhibitor 3 promoted cell proliferation by driving cell cycle from G1 to S phase in esophageal squamous cell carcinoma. *J Cancer* 2019, 10: 1915–1922

39. Peter M. Joining the complex: cyclin-dependent kinase inhibitory proteins and the cell cycle. *Cell* 1994, 79: 181–184

40. Lloyd RV, Erickson LA, Jin L, Kulig E, Qian X, Cheville JC, Scheithauer BW. p27kip1: a multifunctional cyclin-dependent kinase inhibitor with prognostic significance in human cancers. *Am J Pathol* 1999, 154: 313–323

41. Manu KA, Cao PH, Chai TF, Casey PJ, Wang M. p21cip1/waf1 coordinates autophagy, proliferation and apoptosis in response to metabolic stress. *Cancers* 2019, 11: 1112

42. Liu C, Wang X, Shen L. Subcellual localization of p27∼(kip1) and tumour. *Cancer Research on Prevention and Treatment* 2005, 42: 522–525

43. Wang X, Shen QW, Wang J, Zhang Z, Feng F, Chen T, Zhang Y, *et al.* KLF7 regulates satellite cell quiescence in response to extracellular signaling. *Stem Cells* 2016, 34: 1310–1320

44. Chen H, Liu C, Chen C, Su Z, Shu J, Zhang M, Li H, *et al.* Bone morphogenetic protein 4 regulates immortalized chicken preadipocyte proliferation by promoting G1/S cell cycle progression. *FEBS Open Bio* 2019, 9: 1109–1118

45. Zhang J, Cai B, Ma M, Luo W, Zhang Z, Zhang X, Nie Q. ALDH1A1 inhibits chicken preadipocytes' proliferation and differentiation via the PPARγ pathway *in vitro* and *in vivo*. *Int J Mol Sci* 2020, 21: 3150

46. Wang L, Na W, Wang YX, Wang YB, Wang N, Wang QG, Li YM, *et al.* Characterization of chicken *PPARγ* expression and its impact on adipocyte proliferation and differentiation. *Hereditas (Beijing)* 2012, 34: 454–464

47. Zhang Q, Huang JJ, X. YC, Wang YX, Zhang H, Zhao JG, Li H. CRISPR/Cas9 mediated RB1 gene knockout and its function in differentiation and proliferation of chicken preadipocytes. *Acta Veterinaria et Zootechnica Sinica* 2016, 47: 1775–1784

48. Shi HY, Qi HE, Cheng M, Sun YN, Hui LI, Wang NJS. Effect of HOPX gene overexpression on chicken preadipocyte proliferation. *Scientia Agricultura Sinica* 2015, 48: 1624–1631

49. Zhang X, Cheng B, Liu C, Du Z, Zhang H, Wang N, Wu M, *et al.* A novel regulator of preadipocyte differentiation, transcription factor TCF21, functions partially through promoting LPL expression. *Front Physiol* 2019, 10: 458

50. Deng M, Wang J, Chen Y, Zhang L, Xie G, Liu Q, Zhang T, *et al.* Silencing cyclin-dependent kinase inhibitor 3 inhibits the migration of breast cancer cell lines. *Mol Med Rep* 2016, 14: 1523–1530

51. Yu C, Cao H, He X, Sun P, Feng Y, Chen L, Gong H. Cyclin-dependent kinase inhibitor 3 (*CDKN3*) plays a critical role in prostate cancer via regulating cell cycle and DNA replication signaling. *Biomed Pharmaco Ther* 2017, 96: 1109–1118

52. Gong XQ, Tan M, Sheng HY, Xu ML, Zhang M, Xu H, Xia JQ, *et al.* Research progress of cyclin dependent kinase inhibitor 3. *Journal of Science of Teachers' College and University* 2020, 40: 87–91

53. Markman B, Dienstmann R, Tabernero J. Targeting the PI3K/Akt/mTOR pathway-beyond rapalogs. *Oncotarget* 2010, 1: 530–543

54. Dong X, Tang S, Zhang W, Gao W, Chen Y. GPR39 activates proliferation and differentiation of porcine intramuscular preadipocytes through targeting the PI3K/AKT cell signaling pathway. *J Receptors Signal Transduction* 2016, 36: 130–138

55. Gan L, Liu Z, Jin W, Zhou Z, Sun C. Foxc2 enhances proliferation and inhibits apoptosis through activating Akt/mTORC1 signaling pathway in mouse preadipocytes. *J Lipid Res* 2015, 56: 1471–1480

56. Li T, Zhang L, Jin C, Xiong Y, Cheng YY, Chen K. Pomegranate flower extract bidirectionally regulates the proliferation, differentiation and apoptosis of 3T3-L1 cells through regulation of PPARγ expression mediated by PI3K-AKT signaling pathway. *Biomed Pharmaco Ther* 2020, 131: 110769

57. Green CJ, Göransson O, Kular GS, Leslie NR, Gray A, Alessi DR, Sakamoto K, *et al.* Use of Akt inhibitor and a drug-resistant mutant validates a critical role for protein kinase B/Akt in the insulin-dependent regulation of glucose and system A amino acid uptake. *J Biol Chem* 2008, 283: 27653–27667

58. Ross SE, Erickson RL, Hemati N, MacDougald OA. Glycogen synthase kinase 3 is an insulin-regulated C/EBPα kinase. *Mol Cell Biol* 1999, 19: 8433–8441

59. Tokushima Y, Sulistiyanto B, Takahashi K, Akiba Y. Insulin-glucose interactions characterised in newly hatched broiler chicks. *Br Poultry Sci* 2003, 44: 746–751